

Probing the effectiveness: Chiral perturbation theory calculations of low-energy electromagnetic reactions on deuterium

Daniel R. Phillips

Department of Physics and Astronomy, Ohio University, Athens, OH 45701, U. S. A.;
Email: phillips@phy.ohiou.edu.

Abstract. I summarize three recent calculations of electromagnetic reactions on deuterium in chiral perturbation theory. All of these calculations were carried out to $O(Q^4)$, i.e. next-to-next-to-leading order. The reactions discussed here are: elastic electron-deuteron scattering, Compton scattering on deuterium, and the photoproduction of neutral pions from deuterium at threshold.

INTRODUCTION

Effective field theory (EFT) is a technique commonly used in particle physics to deal with problems involving widely-separated energy scales. It facilitates the systematic separation of the effects of high-energy physics from those of low-energy physics. In strong-interaction physics the low-energy effective theory is chiral perturbation theory (χ PT) [1]. Here the low-energy physics is that of nucleons and pions interacting with each other in a way that respects the spontaneously-broken approximate chiral symmetry of QCD. Higher-energy effects of QCD appear in χ PT as non-renormalizable contact operators. The EFT yields amplitudes which can be thought of as expansions in the ratio of nucleon or probe momenta (denoted here by p and q) and the pion mass to the scale of chiral-symmetry breaking, $\Lambda_{\chi\text{SB}}$, which is of order the mass of the ρ meson. The existence of a small parameter $Q = p/\Lambda_{\chi\text{SB}}, q/\Lambda_{\chi\text{SB}}, m_\pi/\Lambda_{\chi\text{SB}}$, means that hadronic processes can be computed in a controlled way.

The momentum scale of binding in light nuclei is of order m_π and so we should be able to calculate the response of such nuclei to low-energy probes using χ PT. The result is a systematically-improvable, model-independent description. Here I will describe a few recent calculations using this approach. Section 2 outlines the χ PT expansion, and sketches the implications of χ PT for calculations of the NN interaction. Section 3 then looks at electron-deuteron scattering in χ PT as a probe of deuteron structure. Section 4 examines the use of Compton scattering on the deuteron as a way to extract neutron polarizabilities. I conclude in Section 5 with a discussion of neutral pion photoproduction on deuterium at threshold. In these last two reactions I will argue that χ PT's successful reproduction of the experimental data is in no small part due to its consistent treatment of the chiral structure of the nucleon and the deuteron.

POWER COUNTING AND DEUTERON WAVE FUNCTIONS

Power counting

Consider an elastic scattering process on the deuteron whose amplitude we wish to compute. If \hat{O} is the transition operator for this process then the amplitude in question is simply $\langle \psi | \hat{O} | \psi \rangle$, with $|\psi\rangle$ the deuteron wave function. In this section, we follow Weinberg [2, 3, 4], and divide the formulation of a systematic expansion for this amplitude into two parts: the expansion for \hat{O} , and the construction of $|\psi\rangle$.

Chiral perturbation theory gives a systematic expansion for \hat{O} of the form

$$\hat{O} = \sum_{n=0}^{\infty} \hat{O}^{(n)}, \quad (1)$$

where we have labeled the contributions to \hat{O} by their order n in the small parameter Q defined above. Eq. (1) is an operator statement, and the nucleon momentum operator \hat{p} appears on the right-hand side. However, the only quantities which ultimately affect observables are expectation values such as $\langle \psi | \hat{p} | \psi \rangle$. For light nuclei this number is generically small compared to $\Lambda_{\chi\text{SB}}$.

To construct $\hat{O}^{(n)}$ one first writes down the vertices appearing in the chiral Lagrangian up to order n . One then draws all of the two-body, two-nucleon-irreducible, Feynman graphs for the process of interest which are of chiral order Q^n . The rules for calculating the chiral order of a particular graph are:

- Each nucleon propagator scales like $1/Q$;
- Each loop contributes Q^4 ;
- Graphs in which both particles participate in the reaction acquire a factor of Q^3 ;
- Each pion propagator scales like $1/Q^2$;
- Each vertex from the n th-order piece of the chiral Lagrangian contributes Q^n .

In this way we see that more complicated graphs, involving two-body mechanisms, and/or higher-order vertices, and/or more loops, are suppressed by powers of Q .

Deuteron wave functions

There remains the problem of constructing a deuteron wave function which is consistent with the operator \hat{O} . Weinberg's proposal was to construct a χ PT expansion in Eq. (1) for the NN potential V , and then solve the Schrödinger equation to find the deuteron (or other nuclear) wave function [2, 3, 4]. Recent calculations have shown that the NN phase shifts can be understood, and deuteron bound-state static properties reliably computed, with wave functions derived from χ PT in this way [5, 6, 7, 8, 9].

Now for χ PT in the Goldstone-boson and single-nucleon sector loop effects are generically suppressed by powers of the small parameter Q . In zero and one-nucleon reactions the power counting in Q applies to the amplitude, and not to the two-particle potential. However, the existence of the deuteron tells us immediately that a power

counting in which loop effects are suppressed cannot be correct for the two-nucleon case, since if it were there would be no NN bound state. Weinberg’s proposal to instead power-count the potential is one response to this dilemma. However, its consistency has been vigorously debated in the literature (see [10, 11] for reviews). Recently Beane *et al.* [12] have resolved this discussion, by showing that Weinberg’s proposal is consistent in the ${}^3S_1 - {}^3D_1$ channel.

One way to understand the χ PT power-counting for deuteron wave functions is to examine the deuteron wave function in three different regions. Firstly, in the region $R \gg 1/m_\pi$ the deuteron wave function is described solely by the asymptotic normalizations A_S, A_D , and the binding energy B . These quantities are observables, in the sense that they can be extracted from phase shifts by an analytic continuation to the deuteron pole.

The second region corresponds to $R \sim 1/m_\pi$. Here pion exchanges play a role in determining the NN potential V , and, associatedly, the deuteron wave functions u and w . The leading effect comes from iterated one-pion exchange—as has been known for at least fifty years. Calculations with one-pion exchange (OPE) defining the potential in this regime will be referred to below as “leading-order” (LO) calculations for the deuteron wave function. Corrections at these distances come from two-pion exchange, and these corrections can be consistently calculated in χ PT. They are suppressed by powers of the small parameter Q , and in fact the “leading” two-pion exchange is suppressed by Q^2 relative to OPE. This two-pion exchange can be calculated from vertices in $\mathcal{L}_{\pi N}^{(1)}$ and its inclusion in the NN potential results in the so-called “NLO” calculation described in detail in Ref. [7]. Corrections to this two-pion-exchange result from replacing one of the NLO two-pion-exchange vertices by a vertex from $\mathcal{L}_{\pi N}^{(2)}$. This results in an additional suppression factor of Q , or an overall suppression of Q^3 relative to OPE, and an “NNLO” chiral potential [5, 6, 7, 8]. More details on this can be found in the contributions of Epelbaum and Timmermans to these proceedings.

Finally, at short distances, $R \ll 1/m_\pi$ we cutoff the chiral one and two-pion-exchange potentials and put in some short-distance potential whose parameters are arranged so as to give the correct deuteron asymptotic properties.

ELASTIC ELECTRON SCATTERING ON DEUTERIUM

One quantitative test of this picture of deuteron structure is provided by elastic electron-deuteron scattering. We thus turn our attention to the deuteron electromagnetic form factors G_C, G_Q , and G_M . These are matrix elements of the deuteron current J_μ , with:

$$G_C = \frac{1}{3e(1+\eta)} (\langle 1 | J^0 | 1 \rangle + \langle 0 | J^0 | 0 \rangle + \langle -1 | J^0 | -1 \rangle), \quad (2)$$

$$G_Q = \frac{1}{M_d^2 2e\eta(1+\eta)} (\langle 0 | J^0 | 0 \rangle - \langle 1 | J^0 | 1 \rangle) \quad (3)$$

$$G_M = \frac{1}{\sqrt{2}\eta(1+\eta)} \langle 1 | J^+ | 0 \rangle \quad (4)$$

where we have labeled these (non-relativistic) deuteron states by the projection of the deuteron spin along the direction of the momentum transfer \mathbf{q} and $\eta \equiv |\mathbf{q}|^2/(4M_d^2)$. G_C, G_Q , and G_M are related to the experimentally-measured A, B , and T_{20} in the usual

way, with T_{20} being primarily sensitive to G_Q/G_C and B depending only to G_M . Here we will compare calculations of the charge and quadrupole form factor with the recent extractions of G_C and G_Q from data [13].

Both of these form factors involve the zeroth-component of the deuteron four-current J^0 . Here we split J^0 into two pieces: a one-body part, and a two-body part. The one-body part of J^0 begins at order Q (where we are counting the proton charge $e \sim Q$) with the impulse approximation diagram calculated with the non-relativistic single-nucleon charge operator for strcutreless nucleons. Corrections to the single-nucleon charge operator from relativistic effects and nucleon structure are suppressed by two powers of Q , and thus arise at $O(Q^3)$, which is the next-to-leading order (NLO) for G_C and G_Q . At this order one might also expect meson-exchange current (MEC) contributions, such as those shown in Fig. 1. However, all MECs constructed with vertices from $\mathcal{L}_{\pi N}^{(1)}$ are isovector, and so the first effect does not occur until N²LO, or $O(Q^4)$, where an $NN\pi\gamma$ vertex from $\mathcal{L}_{\pi N}^{(2)}$ replaces the upper vertex in the middle graph of Fig. 1, and produces an isoscalar contribution to the deuteron charge operator. (This exchange-current contribution was first derived by Riska [14].)

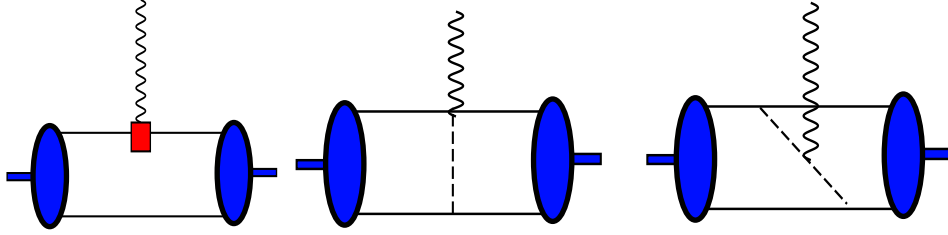


FIGURE 1. The impulse-approximation contribution to G_C and G_Q is shown on the left, while two meson-exchange current mechanisms which would contribute were the deuteron not an isoscalar target are depicted in the middle and on the right.

The most important correction that arises at NLO is the inclusion of *nucleon* structure in χ PT. At $O(Q^3)$ the isoscalar form factors are dominated by short-distance physics, and so the only correction to the point-like leading-order result comes from the inclusion of the nucleon’s electric radius, i.e.

$$G_E^{(s)} \chi\text{PT NLO} = 1 - \frac{1}{6} \langle r_E^{(s)2} \rangle q^2. \quad (5)$$

This description of nucleon structure breaks down at momentum transfers q of order 300 MeV. There is a concomitant failure in the description of eD scattering data [15, 16]. Consequently, in order to focus on *deuteron* structure, in the results presented below I have chosen to circumvent this issue by using a “factorized” inclusion of nucleon structure [16]. This facilitates the inclusion of experimentally-measured single-nucleon form factors in the calculation, thereby allowing us to test how far the theory is able to describe the *two-body* dynamics that takes place in eD scattering.

The results for G_C and G_Q are shown in Fig. 2. The figure demonstrates that convergence is quite good below $q \sim 700$ MeV—especially for G_C . The results shown are for the NLO chiral wave function, but the use of the NNLO chiral wave function, or indeed of simple wave functions which include only one-pion exchange, do not modify the picture greatly below $q = 700$ MeV [16]. It is also clear that—provided information from

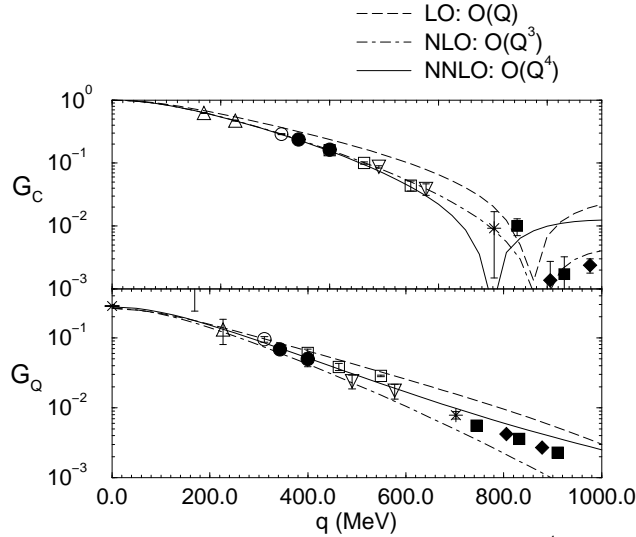


FIGURE 2. The deuteron charge and quadrupole form factors to order Q^4 in chiral perturbation theory. The experimental data is taken from the compilation of Ref. [13]. G_Q is in units of fm^2 .

eN scattering is taken into account— χ PT is perfectly capable of describing the charge and quadrupole form factors of deuterium at least as far as the minimum in G_C . This result is extremely encouraging for the application of EFT to light nuclei.

G_M can be obtained in a similar way, but, importantly, the LO contribution to G_M is $O(Q^2)$. Furthermore, no two-body mechanism enters until $O(Q^5)$, when an undetermined two-body counterterm appears [15, 17]. Results for F_M at $O(Q^4)$ turn out to be of similar quality to those for F_C [15, 16], but are somewhat more sensitive to short-distance physics, as was expected given the presence of the $O(Q^5)$ counterterm in this observable.

The static properties of the deuteron obtained in this expansion are also generically quite reasonable, and have good convergence properties. The one exception to this is the deuteron quadrupole moment, Q_d , which, is underpredicted by about 4%—as is also true in all modern potential-model calculations [18]. However, such an underprediction is not unexpected in χ PT since simple estimates of the effect on Q_d of higher-order terms in the chiral Lagrangian suggest that a discrepancy of order 5% is to be expected at $O(Q^4)$. Q_d is rather sensitive to short-distance physics and it transpires that higher-order counterterms have a larger effect on it than on G_C [19, 20]. This way of understanding the “ Q_d puzzle” is one example of the way in which χ PT can assist in the analysis of electromagnetic currents for few-body systems. For an analogous application of χ PT/EFT ideas to the important solar reaction $pp \rightarrow de^+\nu_e$ see Ref. [21] and the contribution of Marcucci to these proceedings.

COMPTON SCATTERING ON DEUTERIUM

Compton scattering on the nucleon at low energies is a fundamental probe of the long-distance structure of these hadrons. This process has been studied in χ PT in

Ref. [22, 23], where the following results for the proton polarizabilities were obtained at LO:

$$\alpha_p = \frac{5e^2 g_A^2}{384\pi^2 f_\pi^2 m_\pi} = 12.2 \times 10^{-4} \text{ fm}^3; \quad \beta_p = \frac{e^2 g_A^2}{768\pi^2 f_\pi^2 m_\pi} = 1.2 \times 10^{-4} \text{ fm}^3. \quad (6)$$

Recent experimental values for the proton polarizabilities are [24]

$$\begin{aligned} \alpha_p + \beta_p &= 13.23 \pm 0.86_{-0.49}^{+0.20} \times 10^{-4} \text{ fm}^3, \\ \alpha_p - \beta_p &= 10.11 \pm 1.74_{-0.86}^{+1.22} \times 10^{-4} \text{ fm}^3, \end{aligned} \quad (7)$$

where the first error is a combined statistical and systematic error, and the second set of errors comes from the theoretical model employed. These values are in good agreement with the χPT predictions.

Chiral perturbation theory also predicts $\alpha_n = \alpha_p$, $\beta_n = \beta_p$ at this order. The neutron polarizabilities α_n and β_n are difficult to measure, due to the absence of suitable neutron targets, and so this prediction is not well tested. One way to extract α_n and β_n is to perform Compton scattering on nuclear targets. Coherent Compton scattering on a deuteron target has been measured at $E_\gamma = 49$ and 69 MeV by the Illinois group [25] and $E_\gamma = 84.2 - 104.5$ MeV at Saskatoon [26]. The amplitude for Compton scattering on the deuteron clearly involves mechanisms other than Compton scattering on the individual constituent nucleons. Hence, the desire to extract neutron polarizabilities argues for a theoretical calculation of Compton scattering on the deuteron that is under control in the sense that it accounts for *all* mechanisms to a given order in χPT .

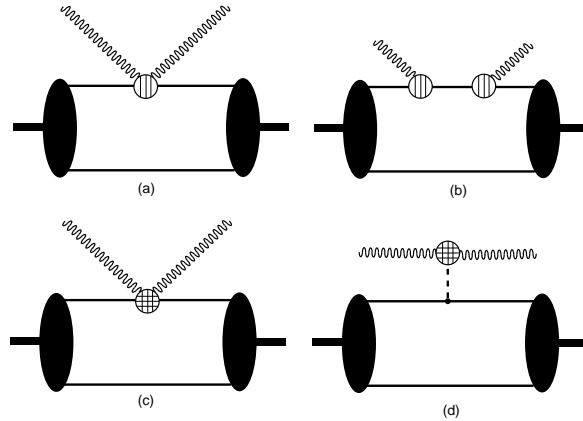


FIGURE 3. Graphs which contribute to Compton scattering on the deuteron at $O(Q^2)$ (a) and $O(Q^3)$ (b-d). The sliced and diced blobs are from $\mathcal{L}_{\pi N}^{(3)}$ (c) and $\mathcal{L}_{\pi\gamma}^{(4)}$ (d). Crossed graphs are not shown.

The Compton amplitude we wish to evaluate is (in the γd center-of-mass frame):

$$\begin{aligned} T_{M'\lambda'M\lambda}^{\gamma d}(\vec{k}', \vec{k}) &= \int \frac{d^3 p}{(2\pi)^3} \Psi_{M'}(\vec{p} + \frac{\vec{k} - \vec{k}'}{2}) T_{\gamma N\lambda'\lambda}(\vec{k}', \vec{k}) \Psi_M(\vec{p}) \\ &+ \int \frac{d^3 p d^3 p'}{(2\pi)^6} \Psi_{M'}(\vec{p}') T_{\gamma NN\lambda'\lambda}^{2N}(\vec{k}', \vec{k}) \Psi_M(\vec{p}) \end{aligned} \quad (8)$$

where M (M') is the initial (final) deuteron spin state, and λ (λ') is the initial (final) photon polarization state, and \vec{k} (\vec{k}') the initial (final) photon three-momentum, which

are constrained to $|\vec{k}| = |\vec{k}'| = \omega$. The amplitude $T_{\gamma N}$ represents the graphs of Fig. 3 and Fig. 4b where the photon interacts with only one nucleon. The amplitude $T_{\gamma NN}^{2N}$ represents the graphs of Fig. 4a where there is an exchanged pion between the two nucleons.

The LO contribution to Compton scattering on the deuteron is shown in Fig. 3(a). This graph involves a vertex from $\mathcal{L}_{\pi N}^{(2)}$ and so is $O(Q^2)$. This contribution is simply the Thomson term for scattering on the proton. There is thus no sensitivity to either two-body contributions *or* nucleon polarizabilities at this order. At $O(Q^3)$ there are several more graphs with a spectator nucleon (Figs. 3(b),(c),(d)), as well as graphs involving an exchanged pion with leading order vertices (Fig. 4(a)) and one loop graphs with a spectator nucleon (Fig. 4(b)) [27]. Graphs such as Fig. 4(b) contain the physics of the proton and neutron polarizabilities at $O(Q^3)$ in χ PT.

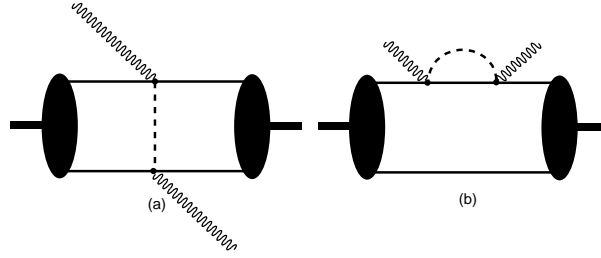


FIGURE 4. Graphs which contribute to Compton scattering on the deuteron at $O(Q^3)$. Crossed graphs are not shown.

We employed a variety of wave functions ψ , and found only moderate wave-function sensitivity. Results shown here are generated with the NLO chiral wave function of Ref. [7]. Fig. 5 shows the results at $E_\gamma = 49, 69,$ and 95 MeV. For comparison we have included the calculation at $O(Q^2)$ in the kernel, where the second contribution in Eq. (8) is zero, and the single-scattering contribution is given solely by Fig. 3(a). At $O(Q^3)$ all contributions to the kernel are fixed in terms of known pion and nucleon parameters, so to this order χ PT makes *predictions* for deuteron Compton scattering. We also show the $O(Q^4)$ result which will be discussed below. The curves indicate that higher-order corrections get larger as ω is increased—as expected.

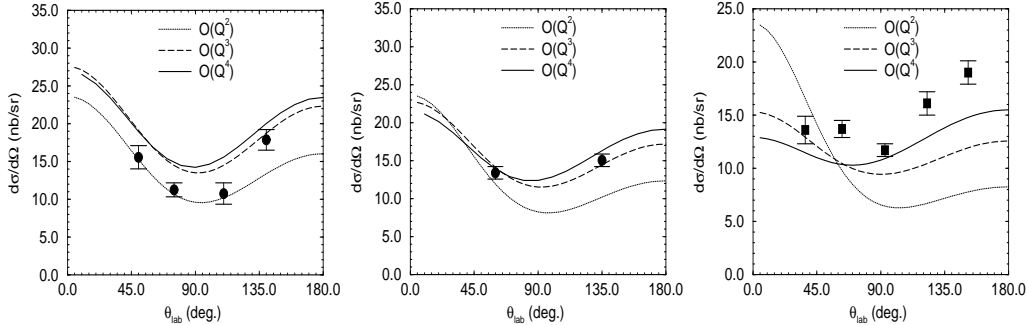


FIGURE 5. Results of the $O(Q^2)$ (dotted line), $O(Q^3)$ (dashed line), and $O(Q^4)$ (solid line) calculations for $E_\gamma = 49$ MeV, 69 MeV and 95 MeV respectively from left to right.

We have also shown the six Illinois data points at 49 and 69 MeV [25] and the Saskatoon data at 95 MeV [26]. Statistical and systematic errors have been added in quadrature. It is quite remarkable how well the $O(Q^2)$ calculation reproduces the 49

MeV data. However, the agreement is somewhat fortuitous: there are significant $O(Q^3)$ corrections. Note that at these lower photon energies Weinberg power counting begins to break down, since it is designed for $\omega \sim m_\pi$, and does *not* recover the deuteron Thomson amplitude as $\omega \rightarrow 0$. Correcting the power counting to remedy this difficulty appears to improve the description of the 49 MeV data, without significantly modifying the higher-energy results [27]. Meanwhile, the agreement of the $O(Q^3)$ calculation with the 69 MeV data is very good, although only limited conclusions can be drawn. These results are not very different from other, potential-model, calculations [28, 29, 30]. They are also quite similar to those obtained in NN EFTs without explicit pions (see Ref. [31], and the contribution of Grißhammer to these proceedings). However our calculation is the only one that does not employ the polarizability approximation for the γN amplitude.

At $O(Q^4)$ single-nucleon counterterms which shift the polarizabilities enter the calculation. However, there are still no two-body counterterms contributing to $\gamma d \rightarrow \gamma d$ at this order. In this sense Compton scattering on deuterium at $O(Q^4)$ is analogous to the reaction $\gamma d \rightarrow \pi^0 d$ discussed below: an $O(Q^4)$ calculation allows us to test the single-nucleon physics which is used to predict the results of coherent scattering on deuterium, since there are no undetermined parameters in the two-body mechanisms that enter to this order in the chiral expansion.

The $O(Q^4)$ plot shown above is a partial calculation at that order. It includes all two-body mechanisms at $O(Q^4)$, and some one-body mechanisms, the latter being calculated in ways motivated by dispersion-relation analyses. The values of the proton polarizabilities used in Fig. 5 were taken from Eq. (7). Meanwhile the (disputed) neutron-atom scattering value of Ref. [32] was employed for α_n and the Baldin sum rule used to fix β_n . To demonstrate the sensitivity to α_n , we can also use the freedom in the single-nucleon amplitude at $O(Q^4)$ to fit the SAL data using the incomplete $O(Q^4)$ calculation. A reasonable fit at backward angles can be achieved with $\alpha_n = 4.4$ and $\beta_n = 10$. These numbers are in startling disagreement with the $O(Q^3)$ χPT expectations. We have also plotted the cross-section at 69 MeV with $\alpha_n = 4.4$ and $\beta_n = 10$: this curve misses the Illinois data. (Similar results were found in a potential model in Ref. [29].) This situation poses an interesting theoretical puzzle. A full $O(Q^4)$ calculation in χPT using the recently derived single-nucleon Compton amplitude [33] is necessary before firm conclusions can be drawn. Such a calculation is in progress [34].

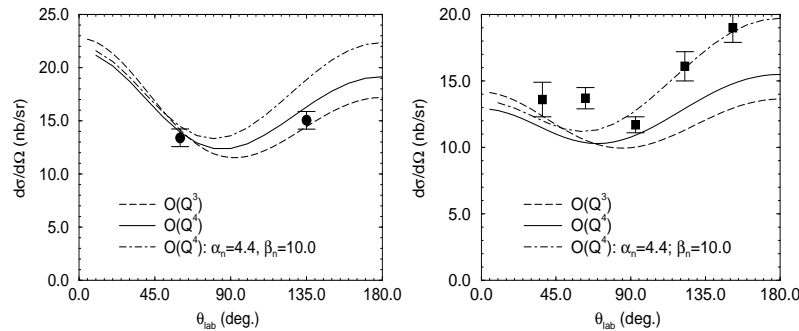


FIGURE 6. Results of $O(Q^3)$ (dashed line), partial $O(Q^4)$ (solid line), and partial $O(Q^4)$ with modified α_n (dot-dashed line), χPT calculations for $E_\gamma = 69$ MeV (left panel) and 95 MeV (right panel).

NEUTRAL PION PHOTOPRODUCTION ON DEUTERIUM

Pion photoproduction on the nucleon near threshold has been studied up to $O(Q^4)$ in χPT with the delta integrated out in Ref. [35]. The differential cross-section at threshold is given solely by E_{0+} , the electric dipole amplitude. In χPT neutral pion photoproduction on the nucleon does not begin until $O(Q^2)$, where there is a tree-level contribution from a $\gamma\pi NN$ vertex. Then at $O(Q^3)$ there are tree-level contributions involving the magnetic moment of the nucleon. The sum of these $O(Q^2)$ and $O(Q^3)$ effects reproduces an old “low-energy theorem”. Also at $O(Q^3)$ there occur finite loop corrections where the photon interacts with a virtual pion which then rescatters on the nucleon. This large quantum effect was missed in the old “low-energy theorem” and is absent in most models. At $O(Q^4)$ there are loops with relativistic corrections, together with a counterterm. The proton amplitude that results from fitting this counterterm to data produces energy-dependence in relatively good agreement with the recent results from Mainz and Saskatoon. At the same order there is also a prediction for the near-threshold behavior of the $\gamma n \rightarrow \pi^0 n$ reaction; the cross-section is considerably larger than that obtained in models that omit the important pion-cloud $O(Q^3)$ diagrams. In fact, the $O(Q^4)$ prediction is that the cross section for $\gamma n \rightarrow \pi^0 n$ is about four times larger than that for neutral pion photoproduction on the proton. A good way to test this prediction is to study neutral pion photoproduction on the deuteron.

If deuterium is to be used as a target in this particular process then two-body mechanisms that contribute to the reaction must be calculated. χPT provides an ideal way to do this, as was demonstrated by Beane and collaborators [36].

Consider the reaction $\gamma(k) + d(p_1) \rightarrow \pi^0(q) + d(p_2)$ in the threshold region, $\vec{q} \simeq 0$, where the pion is in an S wave with respect to the center-of-mass (cm) frame. For real photons the threshold differential cross section is:

$$\left. \frac{|\vec{k}|}{|\vec{q}|} \frac{d\sigma}{d\Omega} \right|_{|\vec{q}|=0} = \frac{8}{3} E_d^2. \quad (9)$$

We now present the results of the chiral expansion of the dipole amplitude E_d to $O(Q^4)$.

Two-body contributions to E_d do not begin until $O(Q^3)$. Thus, to $O(Q^4)$ we have

$$E_d = \langle \Psi | \hat{O}_{ob} | \Psi \rangle + \langle \Psi | \hat{O}_{tb}^{(3)} | \Psi \rangle + \langle \Psi | \hat{O}_{tb}^{(4)} | \Psi \rangle \quad (10)$$

$$\equiv E_d^{ss} + E_d^{tb,3} + E_d^{tb,4}, \quad (11)$$

where we have explicitly isolated the $O(Q^3)$ and $O(Q^4)$ two-body contributions to the operator \hat{O} , and $|\Psi\rangle$ is a deuteron wave function.

The single-scattering contribution to E_d , E_d^{ss} , is given by all diagrams where the photon is absorbed and the pion emitted from one nucleon with the second nucleon acting as a spectator, i. e. the impulse approximation result. Since the χPT results for the elementary S -wave pion production amplitudes to $O(Q^4)$ [35] are known there is an $O(Q^4)$ χPT prediction for E_d^{ss} . This is the prediction we want to test.

But, before comparing this prediction with the experimental data we must compute the two-body contributions to E_d . Those of $O(Q^3)$ which survive at threshold, in the Coulomb gauge, are shown in Fig. 7 [37].

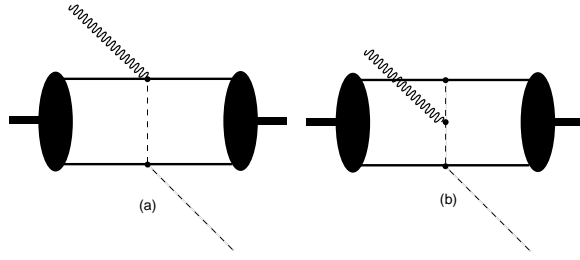


FIGURE 7. Two-nucleon graphs which contribute to neutral pion photoproduction at threshold to $O(Q^3)$ (in the Coulomb gauge). All vertices come from $\mathcal{L}_{\pi N}^{(1)}$.

At $O(Q^4)$, we have to consider the two-nucleon diagrams—some of which are shown in Fig. 8, with the blob characterizing an insertion from $\mathcal{L}_{\pi N}^{(2)}$. There are also relativistic corrections to the graphs in Fig. 7.

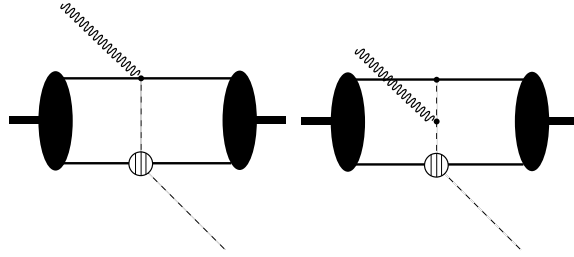


FIGURE 8. Characteristic two-nucleon graphs contributing at $O(Q^4)$ to neutral pion photoproduction. The hatched circles denote an insertion from $\mathcal{L}_{\pi N}^{(2)}$.

One can show that the only terms that survive at threshold result in insertions $\sim 1/2M$, $\sim g_A/2M$ and $\sim \kappa_{0,1}$. To $O(Q^4)$ there are no four-nucleon operators contributing to the deuteron electric dipole amplitude, and so *no new, undetermined parameters appear*. The only free parameter is fixed in $\gamma p \rightarrow \pi^0 p$, and so a genuine *prediction* can be, and was, made for the reaction $\gamma d \rightarrow \pi^0 d$ at threshold.

We now present results. Using a variety of deuteron wave functions the single-scattering contribution is found to be [36]:

$$E_d^{ss} = (0.36 \pm 0.05) \times 10^{-3} / m_{\pi^+}. \quad (12)$$

The sensitivity of the single-scattering contribution E_d^{ss} to the elementary neutron amplitude may be parameterized by:

$$E_d^{ss} = \left[0.36 - 0.38 \cdot (2.13 - E_{0+}^{\pi^0 n}) \right] \times 10^{-3} / m_{\pi^+}. \quad (13)$$

The two-nucleon contribution is evaluated at $O(Q^3)$ using different deuteron wave functions [36]. The results prove to be largely insensitive to the choice of wave function, as do the two-body contributions at $O(Q^4)$. Choosing the AV18 wave function for

definiteness the results are summarized in Table 1¹. The $O(Q^4)$ contributions give corrections of order 15% to the $O(Q^3)$ two-nucleon terms. We also observe that $E_d^{tb,4}$ is of the same size as E_d^{ss} , clearly demonstrating the need to go to this order in the expansion. This gives us confidence that the χ PT expansion is controlled, and that we may compare experimental data with the $O(Q^4)$ prediction [36] :

$$E_d = (-1.8 \pm 0.2) \times 10^{-3} / m_{\pi^+}. \quad (14)$$

TABLE 1. Values for E_d in units of $10^{-3}/m_{\pi^+}$ from one-nucleon contributions ($1N$) up to $O(Q^4)$, two-nucleon kernel ($2N$) at $O(Q^3)$ and at $O(Q^4)$, and their sum ($1N + 2N$).

$1N$	$2N$		$1N + 2N$
$Q + Q^2 + Q^3 + Q^4$	Q^3	Q^4	$Q + Q^2 + Q^3 + Q^4$
0.36	-1.90	-0.25	-1.79

To see the sensitivity to the elementary neutron amplitude, we set the latter to zero and find $E_d = -2.6 \times 10^{-3} / m_{\pi^+}$ (for the AV18 potential). Thus χ PT makes a prediction that differs markedly from conventional models, with that difference arising predominantly from a different result for $E_{0+}^{\pi^0 n}$. An experimental test of this prediction was carried out recently at Saskatoon [38]. The results for the pion photoproduction cross-section near threshold are shown in Fig. 9, together with the χ PT prediction at threshold. The agreement with χ PT to order $O(Q^4)$ is not better than a reasonable estimate of higher-order terms, but χ PT is clearly superior to models. This is compelling evidence of the importance of chiral loops, and also testimony to the consistency and usefulness of χ PT in analyzing low-energy reactions on deuterium.

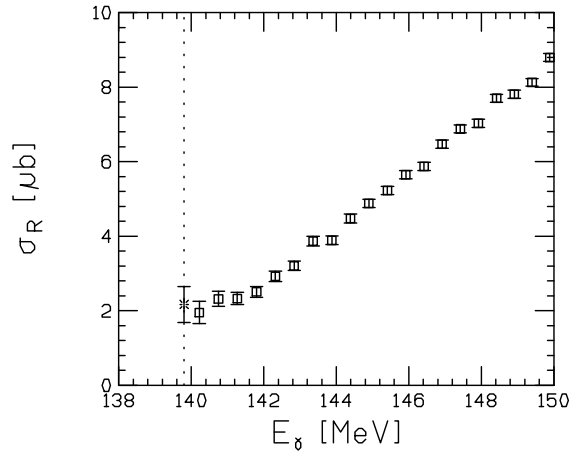


FIGURE 9. Reduced cross-section $\sigma_R = (k/q)\sigma$ in μb for neutral pion photoproduction as function of the photon energy in MeV. Threshold is marked by a dotted line. Squares are data points from Ref. [38] and the star is the χ PT prediction of Ref. [36]. Figure courtesy of Ulf Meißner.

¹ Similar answers were obtained with the wave functions of Ref. [5], which should be equivalent to the NNLO wave function discussed above, up to higher-order terms.

ACKNOWLEDGMENTS

I thank the organizers of “Mesons and Light Nuclei” for an enjoyable meeting. I am also grateful to Silas Beane, Manuel Malheiro, and Bira van Kolck for a profitable and enjoyable collaboration on $\gamma d \rightarrow \gamma d$. Thanks are due to Silas for discussions on $\gamma d \rightarrow \pi^0 d$ and numerous other subjects in effective field theory. Finally, I am grateful to the U. S. Insitute for Nuclear Theory for its hospitality during the writing of this paper.

REFERENCES

1. Bernard, V., Kaiser, N., and Meißner, U.-G., *Int. Jour. of Mod. Phys. E*, **4**, 193 (1995).
2. Weinberg, S., *Phys. Lett.*, **B251**, 288 (1990).
3. Weinberg, S., *Nucl. Phys.*, **B363**, 3 (1991).
4. Weinberg, S., *Phys. Lett.*, **B295**, 114 (1992).
5. Ordonéz, C., Ray, L., and van Kolck, U., *Phys. Rev. C*, **53**, 2086 (1996).
6. Kaiser, N., Brockmann, R., and Weise, W., *Nucl. Phys.*, **A625**, 758 (1997).
7. Epelbaum, E., Glockle, W., and Meißner, U.-G., *Nucl. Phys.*, **A671**, 295 (1999).
8. Rentmeester, M. C. M., Timmermans, R. G. E., Friar, J. L., and de Swart, J. J., *Phys. Rev. Lett.*, **82**, 4992 (1999).
9. Entem, D. R., and Machleidt, R., nucl-th/0107057.
10. van Kolck, U., *Prog. Part. Nucl. Phys.*, **43**, 409 (1999).
11. Beane, S. R., Bedaque, P. F., Haxton, W., Phillips, D. R., and Savage, M. J., in *At the frontier of particle physics—Handbook of QCD*, M. Shifman, ed. (World Scientific, Singapore, 2000).
12. Beane, S. R., Bedaque, P. F., Savage, M. J., and van Kolck, U., nucl-th/0104030.
13. Abbott, D., et al. [JLAB t20 Collaboration] *Eur. Phys. J.*, **A7**, 421 (2000).
14. Riska, D. O., *Prog. Part. Nucl. Phys.*, **11**, 199 (1984).
15. Meißner, U.-G., and Walzl, M., *Phys. Lett.*, **B513**, 37 (2001).
16. Phillips, D. R., in preparation.
17. Park, T.-S., Kubodera, K., Min, D.-P., and Rho, M., *Phys. Lett.*, **B472**, 232 (2000).
18. Carlson, J., and Schiavilla, R., *Rev. Mod. Phys.*, **70**, 743 (1998).
19. Chen, J.-W., Rupak, G., and Savage, M., *Nucl. Phys.*, **A653**, 386 (1999).
20. Phillips, D. R., and Cohen, T. D., *Nucl. Phys.*, **A668**, 45 (2000).
21. Park, T. S., Marcucci, L. E., Viviani, M., Kievsky, A., Rosati, S., Kubodera, K., Min, D.-P., and Rho, M., nucl-th/0106025.
22. Bernard, V., Kaiser, N., and Meißner, U. G., *Nucl. Phys.*, **B383**, 442–496 (1992).
23. Bernard, V., Kaiser, N., Kambor, J., and Meißner, U. G., *Nucl. Phys.*, **B388**, 315–345 (1992).
24. Tonnison, J., Sandorfi, A. M., Hoblit, S., and Nathan, A. M., *Phys. Rev. Lett.*, **80**, 4382–4385 (1998).
25. Lucas, M. A., *Compton scattering from the deuteron at intermediate energies*, Ph.D. thesis, University of Illinois (1994), unpublished.
26. Hornidge, D. L., et al., *Phys. Rev. Lett.*, **84**, 2334–2337 (2000).
27. Beane, S. R., Malheiro, M., Phillips, D. R., and van Kolck, U., *Nucl. Phys.*, **A656**, 367 (1999).
28. Wilbois, T., Wilhelm, P., and Arenhovel, H., *Few Bod. Sys.*, **9**, 263 (1995).
29. Levchuk, M. I., and L’vov, A. I., *Nucl. Phys.*, **A674**, 449 (2000).
30. Karakowski, J. J., and Miller, G. A., *Phys. Rev.*, **C60**, 014001 (1999).
31. Griebhammer, H. W., and Rupak, G., nucl-th/0012096.
32. Schmiedmayer, J., Riehs, P., Harvey, J. A., and Hill, N. W., *Phys. Rev. Lett.*, **66**, 1015 (1991).
33. McGovern, J., *Phys. Rev.*, **C63**, 064608 (2001), and in these proceedings.
34. Beane, S. R., Malheiro, M., McGovern, J., Phillips, D. R., and van Kolck, U., in preparation.
35. Bernard, V., Kaiser, N., and Meißner, U.-G., *Z. Phys.*, **C70**, 483 (1996).
36. Beane, S. R., Bernard, V., Lee, H., Meißner, U.-G., and van Kolck, U., *Nucl. Phys.*, **A618**, 381 (1997).
37. Beane, S. R., Lee, C.-Y., van Kolck, U., *Phys. Rev.*, **C52**, 2914 (1995).
38. Bergstrom, J. C., Igarashi, R., Vogt, J. M., Kolb, N., Pywell, R. E., Skopik, D. M., and Korkmaz, E., *Phys. Rev.*, **C57**, 3203 (1998).